On the Analysis of Peak-to-Average Ratio (PAR) for IS95 and CDMA2000 Systems

Vincent K. N. Lau

***Abstract*—Peak-to-average ratio (PAR) of a signal is an important parameter to a linear amplifier because it determines the *backoff* factor needed to be applied to the amplifier in order to avoid clipping and hence spectral regrowth. In this paper, we analyzed the PAR of the downlink direct code-division multiple-access (DS-CDMA) signal for the IS-95 (2G) and the CDMA2000 (3G) systems. Both the single-carrier (SC) and the multi-carrier (MC) situations are considered. For MC systems, an analytical model is developed to describe the PAR distribution. Closed-form expressions are obtained. Results are compared with simulations, and a nearly exact match is found. This is very useful since simulations for PAR distribution are very costly. Finally, PAR control by *synthesis methods* are proposed, and their effectiveness are discussed.**

I. Introduction

In direct code-division multiple-access (DS-CDMA) systems, the peak-to average-ratio (PAR) of the aggregate signal for multiple users is usually quite high (above 10 dB). This puts a stringent requirement on the power amplifier and reduces the efficiency in the sense that a higher input backoff factor is needed before the peaks in the signal experience significance distortion[1] due to power amplifier nonlinearity. In other words, a more expensive power amplifier is required to cater for the large peaks signal. Moreover, the forward link capacity and coverage of a cellular network is constrained by the available transmitted power at the base station. Hence, the PAR factor of single-carrier DS-CDMA signal is a very important parameter to the system designers and manufacturers. In the third generation wideband CDMA systems (CDMA2000), multi-carrier CDMA is used as an option for the forward link. Therefore, it is also important to study the PAR performance for multi-carrier DS-CDMA. These are addressed in this paper.

PAR analysis for optic-frequency division multiplexing (OFDM) has appeared in [1]–[6]. However, the PAR behavior of DS-CDMA is quite different from that of OFDM.[2] [7] investigated the PAR analysis of single carrier DS-CDMA signals by simulation based on IS95 specification. In this paper, we contribute in the following ways.

- Define and relate the PAR behavior to ergodicity of the random process. This enables us to formulate an analytical model for the PAR of multi-carrier signals.
- Analyze the PAR for both single-carrier (SC) and multi-carrier (MC) CDMA signals. In particular, we studied the impact of correlation of data traffic and pilot tones on the PAR of multi-carrier CDMA. We also explain the observed phenomena (on field test) where the PAR of CDMA signals is increased when several carriers are combined together.
- Compare and explain the PAR performance between IS95 and CDMA2000 signals [8]. In particular, we explain the observed phenomena where the PAR of single-carrier CDMA2000 signals is always lower than the PAR of single-carrier IS95 signals.
- Present a novel analytical model for the PAR analysis of multi-carrier CDMA signals. This is very useful to avoid costly simulation and to help us to gain insights and perform optimization of the PAR.
- Present a novel algorithm for the optimal selection of walsh codes to minimize the PAR of single carrier CDMA signals which is applicable to both IS95 and CDMA2000 systems.

This paper is organized as follows. In Section II, we give the general background and definition of PAR. In Section III, we study the PAR dependency on walsh code selections for single-carrier IS95 and CDMA2000 systems. In Section IV, we study the multi-carrier situation. Analytical expressions to model the histogram or the probability density function (pdf) of the envelope distribution are found and compared with simulation results. Finally, solutions to reduce PAR for CDMA downlink signals are discussed in Section V. We conclude with a brief summary of results in Section VI.

II. General PAR Definition

We shall first define the peak. Intuitively, a peak of a signal $x(t)$ is given by the maximum of its envelope, $|x(t)|$. However, for a continuous random process, $\max[x(t)]$ could reach infinity provided that the observation interval is long enough. Even for random process with discrete values where $\max\ |x(t)|$ is bounded, it may occur at very low probability which is not very useful in practice [9]. Therefore, a more useful definition of peak is in probability terms given by:

Definition 1: A signal $x(t)$ is said to have a peak at x_p at *cut-off probability* P_c if

$$\Pr[|x(t)| < x_p] = P_c. \tag{1}$$

Manuscript received April 27, 1999; revised October 12, 1999.

The author is with the Department of Electrical and Electronic Engineering, University of Hong Kong, Pokfulam Road, Hong Kong (e-mail: knlau@eee.hku.hk).

Publisher Item Identifier S 0018-9545(00)07911-1.

[1]Distortion in peaks will cause undesirable spectral regrowth in the adjacent bands.

[2]For example, each carrier is modulated by a binary bit in OFDM, whereas each carrier in a multi-carrier CDMA system is modulated by a random process of essentially continuous values.

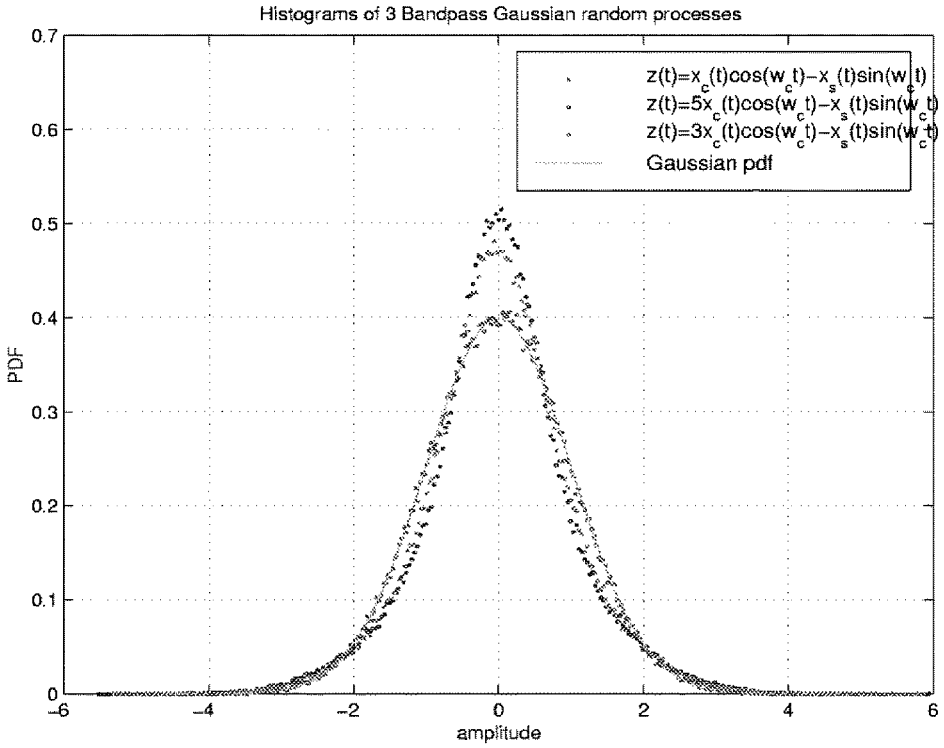

Fig. 1. Distortions of pdf due to different degree of I/Q imbalance

Therefore, the PAR of a random process $x(t)$ could be completely specified by its histogram. The PAR definition in (1) refers to the pdf (or histogram) generated from its time samples.[3] For an ergodic random process, its pdf in time domain and ensemble domain are identical. Otherwise, the histogram (or pdf) in time domain and ensemble domain are in general different and we always refer to the time domain pdf. If an operation is performed on $x(t)$, the PAR of the output will be changed iff its pdf is also changed by the operation. The following gives examples of how the output PAR could be affected by some operations.

Example 1: Let $x_1(t)$ and $x_2(t)$ be two uncorrelated, stationary Gaussian processes, then $x_1(t) + x_2(t)$ will have the same peak-to-average ratio because $x_1(t) + x_2(t)$ is still a stationary Gaussian process and the distribution (across the time domain) is unchanged (Gaussian). Therefore, we have a constant PAR ratio.

Example 2: Let $x_c(t)$ and $x_s(t)$ be two uncorrelated, stationary Gaussian processes (unit variance, zero mean). Consider the general BP Gaussian process:

$$z_{BP}(t) = \alpha_c x_c(t)\cos(\omega_0 t) - \alpha_s x_s(t)\sin(\omega_0 t). \qquad (2)$$

Unless $\alpha_c = \alpha_s$, the random process is not stationary and, hence, is not ergodic. If we collect N samples over an observation time, we could produce a histogram of $\{z_{BP}(t_i)\}$. Because of the nonergodic nature of $z_{BP}(t)$, the histogram (pdf across the time domain) will be distorted from a Gaussian pdf, resulting in a different peak-to-average ratio (increased) compared with a regular Gaussian distribution. This is illustrated in Fig. 1. In another words, the PAR of $z_{BP}(t)$ is a function of α_c/α_s, the amount of I/Q imbalance.

[3]Collect N samples of $x(t)$ and plot its histogram. pdf is resulted as N tends to infinity.

III. PAR for Single Carrier

A. Walsh Code Dependency

Without loss of generality, consider a coded bit duration T_b. The complex envelope of a CDMA downlink signal could be modeled by

$$\tilde{s}(t) = \sum_{l=1}^{L} (\lambda_l PN_I(l) + j\lambda_l PN_Q(l))p(t - lT_c) \qquad (3)$$

where L is the number of chips per T_b, λ_l is defined as the *digital transmission sequence* given by

$$\lambda_l = \sum_{n=0}^{N_u - 1} d_n w_n(l) \qquad (4)$$

N_u is the number of users, d_n = traffic data bit for user-n, $w_n(l)$ is the lth chip of walsh code assigned to user-n, PN_I and PN_Q are the pseudo-random short codes, and $p(t)$ is the transmission pulse shape. Index l is used to indicate chip interval and index n is used to indicate the nth user.

λ_l depends only on the choice of walsh codes and the applied data bits $\{d_n\}$. Due to the band-limited nature of the channel, the pulse width of $p(t)$ will generally span over several chip intervals, causing inter-chip interference at instants other than the ideal sampling times. Because of the inter-chip interference,

and the fact that different users share the same PN sequence, a certain combination of walsh codes and data bits could result in a particular *digital transmission sequence*, λ_l, that has a higher peak compared with the others. Let us illustrate the above idea with the following cases using the transmit pulse as specified in IS95.

Consider two different walsh code sets given by

- Walsh code set 1 = $\{w_0, w_{32}, w_{16}, w_{48}\}$, $d_n(1) = \{1, 1, 1, 1, 1\}$.
- Walsh code set 2 = $\{w_0, w_1, w_{33}, w_{49}\}$, $d_n(2) = \{1, 1, 1, 1, 1\}$.

The overall digital transmission sequences $\lambda_l(1)$ and $\lambda_l(2)$ are shown in Fig. 2(a) and (b) respectively.

Because of the consecutive peaks at $l = 14$, 15 and 16, the transmit pulse, $p(t)$, would overlap and add constructively with each other, resulting in a high peak for walsh set 1 as shown in Fig. 3(a). On the other hand, the previous *bad combination* of consecutive peaks are broken in the walsh set 2 and the resulting peak of the transmitted signal is smaller as shown in Fig. 3(b). This explains the reason for the walsh code dependency of PAR.

B. Comparison Between IS95 and CDMA2000 Systems

Consider a 3G-1X system,[4] the complex envelope of the CDMA2000 forward link signal could be modeled as:

$$\tilde{s}(t) = \sum_{l=1}^{L} (\lambda_l^{(I)} + j\lambda_l^{(Q)})(PN_I(l) + jPN_Q(l))p(t - lT_c) \quad (5)$$

where $\lambda_l^{(I)}$ and $\lambda_l^{(Q)}$ are given by

$$\lambda_l^{(I)} = \sum_{n=0}^{N_u-1} d_n^{(I)} w_n(l) \quad \lambda_l^{(Q)} = \sum_{n=0}^{N_u-1} d_n^{(Q)} w_n(l). \quad (6)$$

3G1X system uses QPSK modulation with complex spreading.[5] QPSK is used to increase the modulation throughput while complex spreading is used to maintain I–Q signal balance. It is shown by simulation that CDMA2000 system has a lower PAR value compared with IS95 system at any fixed walsh code selection (see Fig. 8 in Section V). It would be shown in the following that the PAR reduction is due to QPSK and complex spreading used in CDMA2000 system.

1) PAR Reduction Due to QPSK: For a IS95 system down-link signal, BPSK is employed and the I and Q signals are given by

$$\tilde{s}_I(t) = \sum_l \lambda_l PN_I(l) p(t - lT_c)$$
$$\tilde{s}_Q(t) = \sum_l \lambda_l PN_Q(l) p(t - lT_c). \quad (7)$$

Since PN_I and PN_Q are independent pseudo-random binary sequences $\{+1, -1\}$, they just toggle the sign of the peaks. Peak position is totally determined by the *digital transmission sequence*. Hence, for a particular set of data bits $\{d_n\}$ that causes λ_l (and hence the I-signal) to *peak* at chip position l, the Q-signal, being affected by the same λ_l, is very likely to be large in magnitude at the same chip position. In another words, the I and Q signals are highly correlated in magnitude. This could be illustrated by the I–Q plot of the IS95 CDMA complex envelope in Fig. 4.

To isolate the effect of QPSK, we consider applying QPSK alone with real spreading. When QPSK is applied, the I and Q signals are essentially the same as (5) except the signature λ_l is different for I and Q branches. $\lambda_l^{(I)}$ is determined by the data bits $\{d_n^{(I)}\}$ while $\lambda_l^{(Q)}$ is determined by the data bits $\{d_n^{(Q)}\}$. Because $\{d_n^{(I)}\}$ and $\{d_n^{(Q)}\}$ are independent, a peak for the I-signal at chip-l [caused by $\lambda_l^{(I)}$] is independent of a peak for the Q-signal which is caused by $\lambda_l^{(Q)}$. In another words, the magnitude of I and Q signals become uncorrelated when QPSK is applied. This could be illustrated by the spherical shape of the I–Q *cloud* in Fig. 4.

The overall peak of the complex envelop is given by $\sqrt{(\tilde{s}_I^2(t) + \tilde{s}_Q^2(t))}$. A large peak will occur only when both the I and Q signals are large in magnitude. For the IS95 system, suppose the I signal *peaks* with a certain probability (say P_c). Since I and Q signals are heavily correlated, a large *overall peak* will occur at a probability of about P_c. When QPSK is applied, I and Q signals are uncorrelated and the probability the same peak to occur becomes approximately $P_c \times P_c$ which is highly unlikely. Therefore, only some low density green spots are observed near the peaks of the IS95 system in Fig. 4.

2) PAR Reduction Due to Complex Spreading: When QPSK with complex spreading is applied, the I and Q signals are given by

$$\tilde{s}_I(t) = \sum_l \left(\lambda_l^{(I)} PN_I(l) - \lambda_l^{(Q)} PN_Q(l)\right) p(t - lT_c)$$
$$\tilde{s}_Q(t) = \sum_l \left(\lambda_l^{(I)} PN_Q(l) + \lambda_l^{(Q)} PN_I(l)\right) p(t - lT_c). \quad (8)$$

In general, the gains applied to the I-channel data and the Q-channel data are different. The I-signal power and the Q-signal power are given by

$$\sigma_I^2 = \lim_{T\to\infty} \frac{1}{T} \int_{-T/2}^{T/2} \tilde{s}_I^2(t)\, dt$$
$$= \mathcal{E}\left[\left(\lambda_l^{(I)} PN_I(l)\right)^2\right] + \mathcal{E}\left[\left(\lambda_l^{(Q)} PN_Q(l)\right)^2\right]$$
$$- \mathcal{E}\left[\left(\lambda_l^{(I)} \lambda_l^{(Q)} PN_I(l) PN_Q(l)\right)\right] \quad (9)$$

and

$$\sigma_Q^2 = \lim_{T\to\infty} \frac{1}{T} \int_{-T/2}^{T/2} \tilde{s}_Q^2(t)\, dt$$
$$= \mathcal{E}\left[\left(\lambda_l^{(I)} PN_I(l)\right)^2\right] + \mathcal{E}\left[\left(\lambda_l^{(Q)} PN_Q(l)\right)^2\right]$$
$$+ \mathcal{E}\left[\left(\lambda_l^{(I)} \lambda_l^{(Q)} PN_I(l) PN_Q(l)\right)\right] \quad (10)$$

where $\mathcal{E}(.)$ is the expectation operator. Since PN_I and PN_Q are uncorrelated pseudo-random sequences, the third terms in

[4]3G 1X system refers to cdma2000 with 1.25 MHz bandwidth.

[5]*Real spreading* refers to spreading the I-data signal with PN_I and the Q-data signal with PN_Q. This is used in the IS95 system. *Complex spreading* refers to spreading the complex data $(I + jQ)$ with a complex spreading sequence $(PN_I + jPN_Q)$. This is employed in CDMA2000 design.

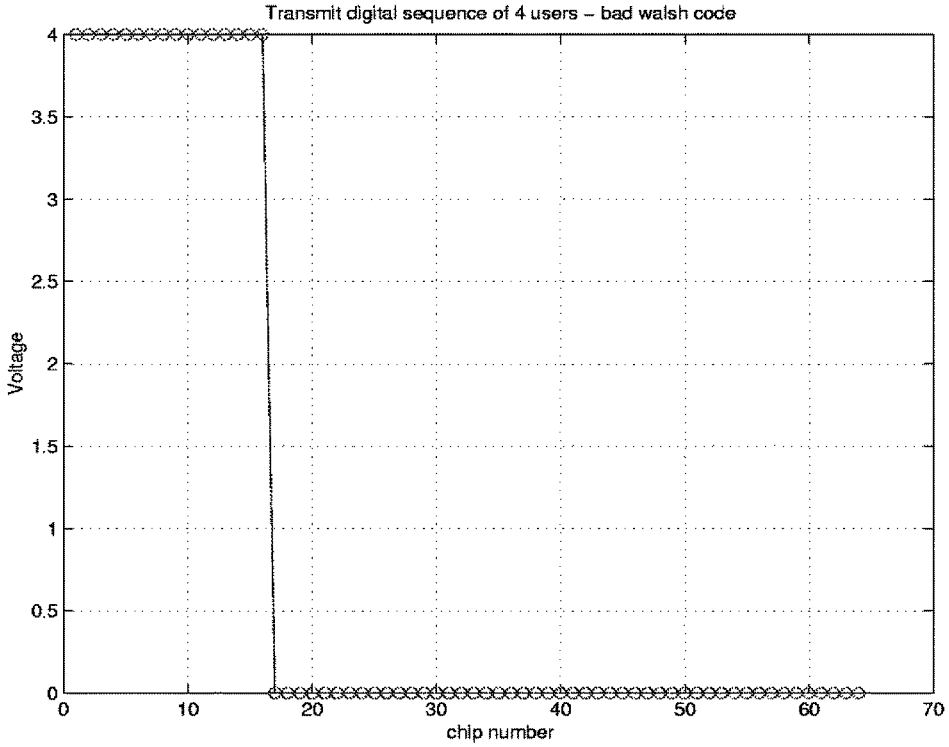

(a)

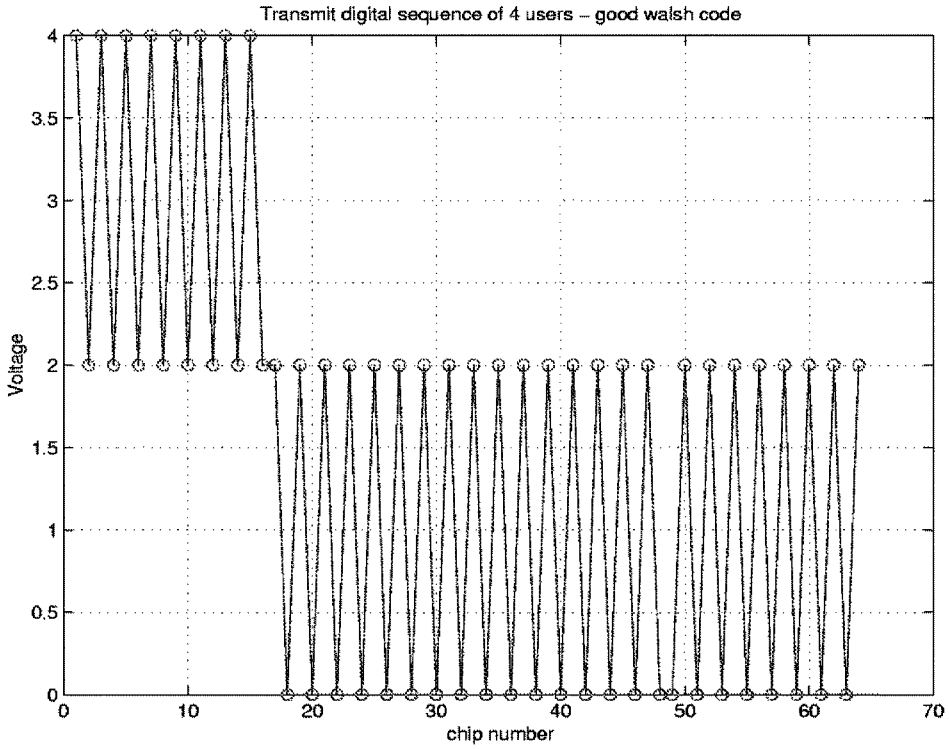

(b)

Fig. 2. An illustration of a good and a bad walsh code combination.

σ_I^2 and σ_Q^2 are zero. Hence, $\sigma_I^2 = \sigma_Q^2$ and one important benefit of complex spreading is to remove the I–Q unbalance that would otherwise occur. As explained in Section II, I–Q imbalance is undesirable because it could raise PAR due to the loss of ergodicity.

IV. PAR FOR MULTI-CARRIER

As mentioned in Section II, the necessary and sufficient condition for a change in PAR is the change or *distortion* of the histogram (or pdf) of a signal. In this section, we propose a

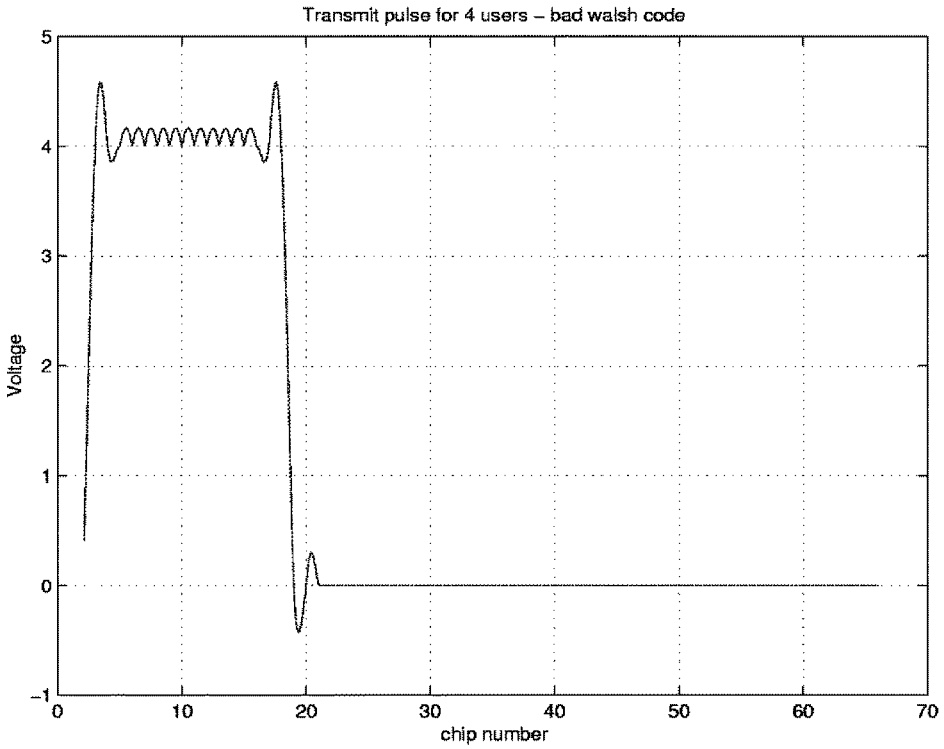

(a)

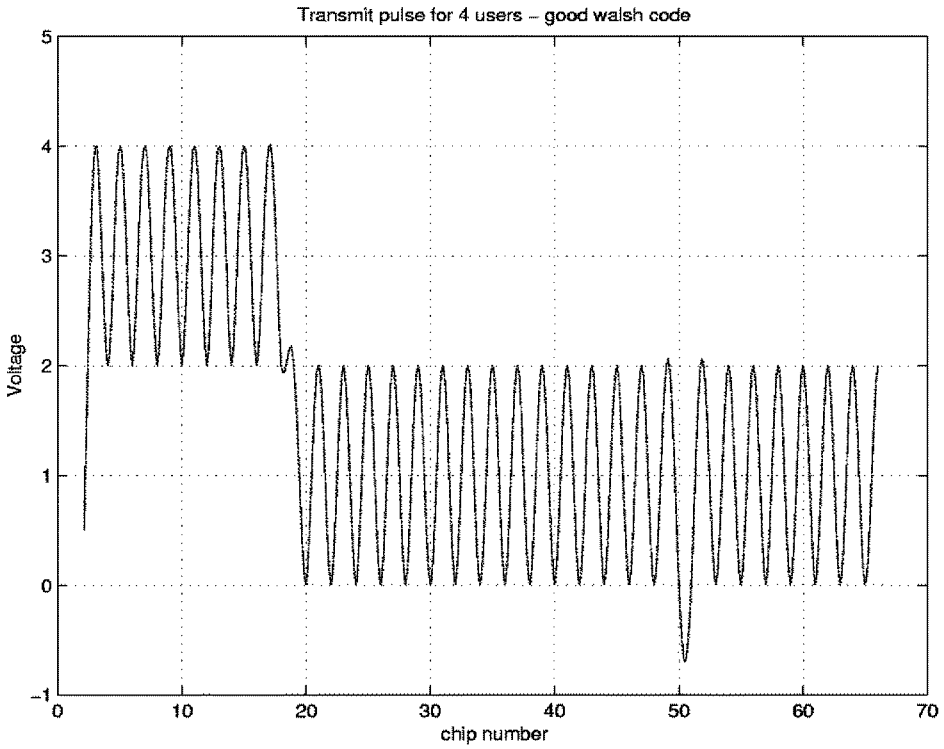

(b)

Fig. 3. Transmitted baseband signal of a good and a bad walsh code combination.

mathematical model so as to describe the PAR change by analytical formulae. To do that, several assumptions are made to simplify the analysis and the results are compared with simulations. The resulting expression could help us to gain insight into the problem and avoid costly simulations. We shall firstly introduce the following theorem.

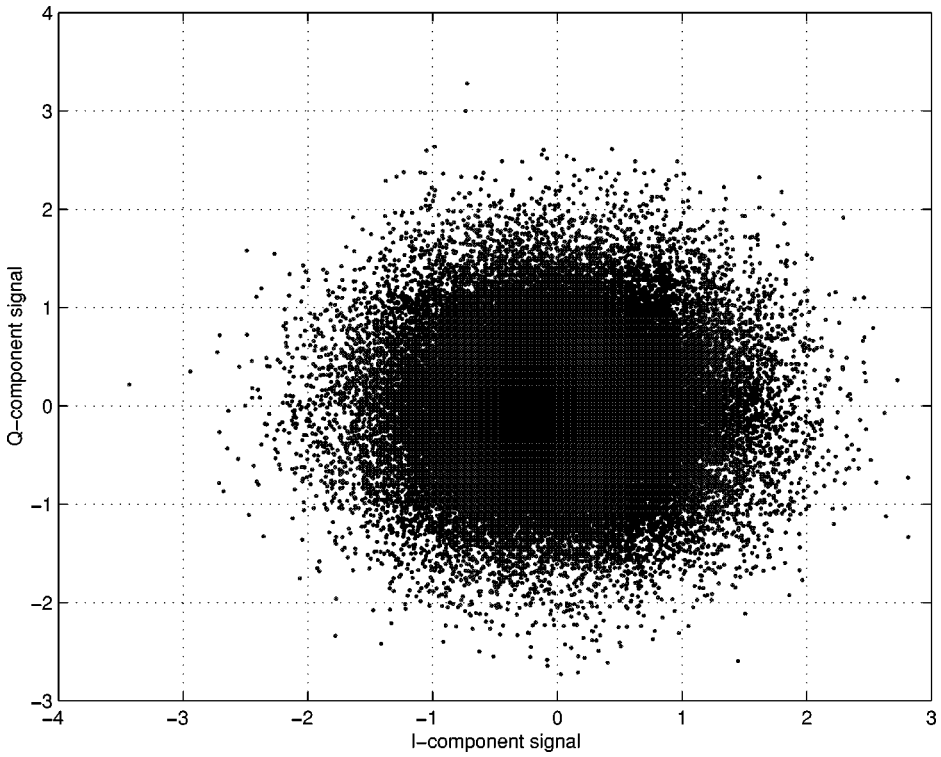

Fig. 4a. Complex plot of I–Q signals for BPSK-real spread (IS95) [red], QPSK-real spread [green], and QPSK-complex spread (CDMA2000) [pink]. Signals are normalized to have the same rms power.

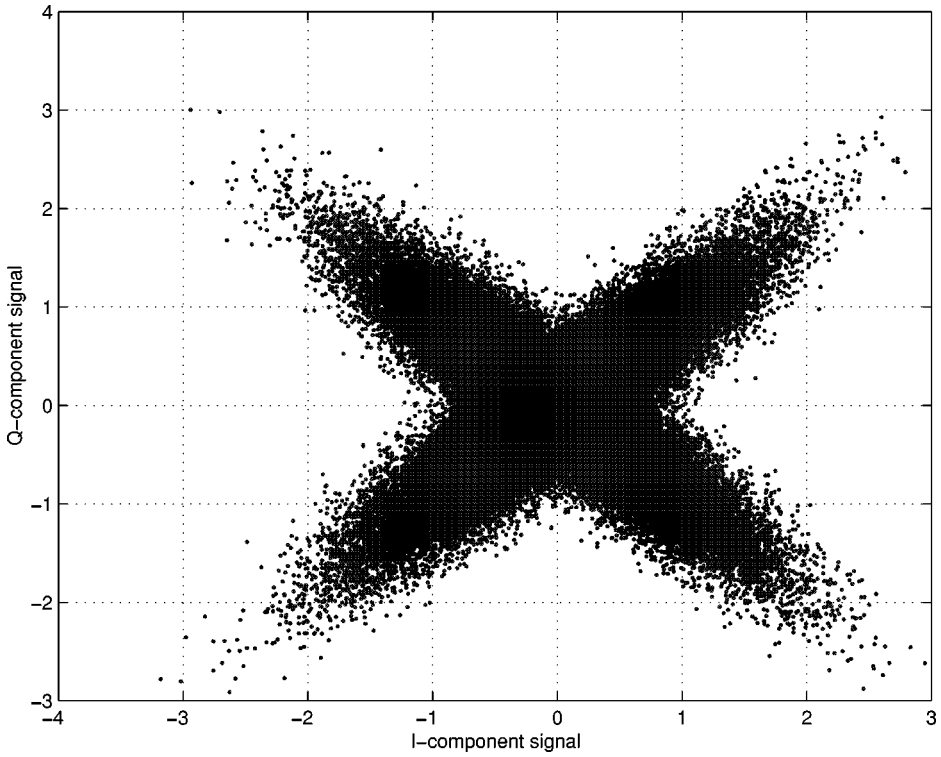

Fig. 4b. Complex plot of I–Q signals for BPSK-real spread (IS95) [red], QPSK-real spread [green], and QPSK-complex spread (CDMA2000) [pink]. Signals are normalized to have the same rms power.

Theorem 1: Let $\{\tilde{x}_1(t), \tilde{x}_2(t), \ldots, \tilde{x}_{N_c}(t)\}$ be a set of N_c complex low-pass random processes and $\tilde{s}(t)$ be the N_c carriers combined complex signal given by

$$\tilde{s}(t) = \tilde{x}_1(t)e^{j(\omega_1 t+\theta_1)} + \tilde{x}_2(t)e^{j(\omega_2 t+\theta_2)} + \cdots + \tilde{x}_{N_c}(t)e^{j(\omega_{N_c} t+\theta_{N_c})} \tag{11}$$

where ω_k and θ_k are the kth combining frequency and phase. Let f_s be the sampling frequency such that

$$\frac{f_1}{f_s} = \frac{P_1}{Q_1}, \quad \frac{f_2}{f_s} = \frac{P_2}{Q_2} \cdots \frac{f_{N_c}}{f_s} = \frac{P_{N_c}}{Q_{N_c}} \tag{12}$$

where P_i and Q_i are relatively prime and $Q = LCM\{Q_1, Q_2, \ldots, Q_{N_c}\}$. If $\tilde{x}_k(t)$ is ergodic for all k, then the histogram or pdf derived from the time samples of $|\tilde{s}(t)|$ is given by

$$f_{|\tilde{s}|}(\alpha) = \frac{1}{Q}\left[\sum_{q:\ |\tilde{s}_q|\neq 0} f_q(\alpha) + \sum_{q:\ |\tilde{s}_q|=0} \delta(\alpha)\right] \tag{13}$$

where $f_q(\alpha)$ is the pdf (in ensemble sense) of $|\tilde{s}_q| = |\tilde{s}(t_{q,n})|$ with $t_{q,n} = nQ+q$, $q \in [1, Q]$, $\delta(\alpha)$ is the Diarc delta function and α is the amplitude level of the complex envelop of the signal $\tilde{s}(t)$.

Proof: Suppose we collect NQ samples from $\tilde{s}(t)$. To derive the histogram for these NQ samples, we divide the samples into Q subsets, each having N samples in such a way that subset-q consists of $\tilde{s}(t)$ sampled at $t_{q,n} = nQ + q\{n = [1, N], q = [1, Q]\}$. Note that, within the subset q, the samples are given by

$$\begin{aligned}\tilde{s}_q(n) &= \tilde{x}_1(t_{q,n})e^{j((2\pi P_1/Q_1)(nQ+q)+\theta_1)} + \tilde{x}_2(t_{q,n})e^{j((2\pi P_2/Q_2)(nQ+q)+\theta_2)} + \cdots \\ &= \tilde{x}_1(t_{q,n})e^{j((2\pi P_1 q/Q_1+\theta_1)} + \tilde{x}_2(t_{q,n})e^{j((2\pi P_2 q/Q_2)+\theta_2)} + \cdots.\end{aligned} \tag{14}$$

Observe that all the complex sinusoid are independent of n and they are just scaling factors. Hence, all samples within the subset q corresponds to a complex ergodic random process. This means that the pdf or histogram of the samples in subset-q alone is identical to the pdf in ensemble sense. Let the individual pdf (in ensemble sense) of subset q be $f_{|\tilde{s}_q|}(\alpha)$ or just $f_q(\alpha)$. The pdf $f_{|\tilde{s}|}(\alpha)$ is given by

$$\begin{aligned}f_{|\tilde{s}|}(\alpha) &= \lim_{\Delta s\to 0}\left\{\frac{1}{\Delta s}\lim_{N\to\infty}\left[\frac{N_{\{||\tilde{s}|-\alpha|<\Delta s\}}}{NQ}\right]\right\} \\ &= \lim_{\Delta s\to 0}\left\{\frac{1}{\Delta s}\lim_{N\to\infty}\left[\frac{\sum_{q=1}^{Q} N_{\{||\tilde{s}_q|-\alpha|<\Delta s\}}}{NQ}\right]\right\} \\ &= \lim_{\Delta s\to 0}\left\{\frac{1}{Q}\sum_q \frac{1}{\Delta s}\lim_{N\to\infty}\left[\frac{N_{\{|\tilde{s}_q|-\alpha|<\Delta s\}}}{N}\right]\right\} \\ &= \frac{1}{Q}\left[\sum_{q:\ |\tilde{s}_q|\neq 0} f_q(\alpha) + \sum_{q:\ |\tilde{s}_q|=0}\delta(\alpha)\right].\end{aligned} \tag{15}$$

□

A. Application to CDMA2000 Systems

As described above, $\tilde{x}_i(t)$ is the complex baseband signal of the DS-CDMA signal for carrier i. Because all CDMA carriers share the same common pilot and different carriers use the same PN_I and PN_Q, there would be correlations between baseband signals $\tilde{x}_i(t)$ and $\tilde{x}_j(t)$. In general, since the pilot component is *deterministic*, it could be taken out and $\tilde{x}_i(t)$ could be expressed as the sum of a deterministic component and a zero-mean random process

$$\begin{aligned}\tilde{x}_i(t) &= \psi_0^{(i)}(PN_I(t) + jPN_Q(t)) + \sum_{n=1}^{N_u}\psi_n^{(i)}w_n^{(i)}(t)\left[d_{n,c}^{(i)}(t) + jd_{n,s}^{(i)}(t)\right] \times [PN_I(t) + jPN_Q(t)] \\ &= \psi_0^{(i)}(PN_I(t) + jPN_Q(t)) + \tilde{x}_i'(t)\end{aligned} \tag{16}$$

where $\psi_n^{(i)}$ and $\{d_{n,c}^{(i)}, d_{n,s}^{(i)}\}$ are the transmitted digital gain and the $[I, Q]$ data bits for carrier-i user-n respectively. Because of QPSK, $d_{n,c}^{(i)}$ and $d_{n,s}^{(j)}$ are uncorrelated. To include the effect of the correlation between traffic data bits of different carriers, we assume $\{d_{n,c}^{(i)}, d_{n,c}^{(j)}\}$ and $\{d_{n,s}^{(i)}, d_{n,s}^{(j)}\}$ are equally correlated [as shown in (17)]. At large N_u, the random component, $\tilde{x}_i'(t)$, could be approximated by a zero-mean complex stationary Gaussian process. To simplify the expression, we assume that all carriers are equally loaded and, hence, $\mathcal{E}[|\tilde{x}_i'(t)|^2] = \mathcal{E}[|\tilde{x}_j'(t)|^2] = 2\sigma_0^2$. Therefore, we have

$$\begin{aligned}&\mathcal{E}[\tilde{x}_{i,c}'\tilde{x}_{j,s}'] = 0, \\ &\mathcal{E}[(\tilde{x}_{i,c}')^2] = \mathcal{E}[(\tilde{x}_{i,s}')^2] = \sigma_0^2 = 2\sum_{n=1}^{N_u-1}(\psi_n^{(i)})^2 \\ &\mathcal{E}[\tilde{x}_{i,c}'\tilde{x}_{j,c}'] = \mathcal{E}[\tilde{x}_{i,s}'\tilde{x}_{j,s}'] = \sigma_0^2\rho \qquad \forall\, i \neq j.\end{aligned} \tag{17}$$

Consider taking $4NQ$ time samples from $\tilde{s}(t)$ and subdivide the samples into Q subsets with Q defined in Theorem 1. The real part and the imaginary part of the signal samples in subset q are given by

$$\begin{aligned}\Re[\tilde{s}_q(n)] &= \sum_{m=1}^{N_c}\left[\psi_0^{(m)}\left(PN_I(t_{q,n})\cos\left(\frac{2\pi P_m}{Q_m}q+\theta_m\right) - PN_Q(t_{q,n})\sin\left(\frac{2\pi P_m}{Q_m}q+\theta_m\right)\right)\right] \\ &\quad + \sum_{m=1}^{N_c}\left[\tilde{x}_{m,c}'(t_{q,n})\cos\left(\frac{2\pi P_m}{Q_m}q+\theta_m\right) - \tilde{x}_{m,s}'(t_{q,n})\sin\left(\frac{2\pi P_m}{Q_m}q+\theta_m\right)\right]\end{aligned} \tag{18}$$

$$\begin{aligned}\Im[\tilde{s}_q(n)] &= \sum_{m=1}^{N_c}\left[\psi_0^{(m)}\left(PN_I(t_{q,n})\sin\left(\frac{2\pi P_m}{Q_m}q+\theta_m\right) + PN_Q(t_{q,n})\cos\left(\frac{2\pi P_m}{Q_m}q+\theta_m\right)\right)\right] \\ &\quad + \sum_{m=1}^{N_c}\left[\tilde{x}_{m,c}'(t_{q,n})\sin\left(\frac{2\pi P_m}{Q_m}q+\theta_m\right) + \tilde{x}_{m,s}'(t_{q,n})\cos\left(\frac{2\pi P_m}{Q_m}q+\theta_m\right)\right],\end{aligned} \tag{19}$$

Within each subset-q, the $4N$ samples could be further subdivided into four smaller subsets of N samples, each corresponding to $\{PN_I, PN_Q\} = \{1, 1\}, \{1, -1\}, \{-1, 1\}$ and $\{-1, -1\}$. Each of these smaller subset is labeled by $p \in [1, 4]$. For these N samples in each of these subsets, their real and imaginary parts, $\Re[\tilde{s}_{q,p}]$ and $\Im[\tilde{s}_{q,p}]$ could be modeled by 2 independent Gaussian processes with means, $[\mu_{q,p}(c), \mu_{q,p}(s)]$, given by the first summation terms of (18) and (19) and variance $[\Sigma_q^2]$ given by

$$\begin{aligned}\Sigma_q^2 &\stackrel{\text{def}}{=} \mathcal{E}[\Re(\tilde{s}_{q,p})^2] \\ &= \mathcal{E}[\Im(\tilde{s}_{q,p})^2] \\ &= N_c\sigma_0^2 + 2\sigma_0^2\rho \sum_{i=1}^{N_c} \sum_{\substack{j=1 \\ j>i}}^{N_c} \cos \\ &\quad \cdot \left(2\pi q\left(\frac{P_i}{Q_i} - \frac{P_j}{Q_j}\right) + (\theta_i - \theta_j)\right). \end{aligned} \tag{20}$$

Note that, in the ideal case when traffic data bits are uncorrelated between different carriers, $\Sigma_q^2 = N_c\sigma_0^2 \; \forall \; q$.

The envelope $|\tilde{s}_{q,p}(n)|$ is given by $\sqrt{[\Re(\tilde{s}_{q,p})^2 + \Im(\tilde{s}_{q,p})^2]}$ which is the square root of the sum of the square of two *independent* but nonzero mean Gaussian variables. Hence, the pdf of the envelope $f_{q,p}(\alpha)$ is Rician distributed and is given by

$$f_{q,p}(\alpha) = \frac{\alpha}{\Sigma_q^2} e^{-[(\alpha^2 + \gamma_{q,p}^2/2\Sigma_q^2)]} I_0\left[\frac{\alpha\gamma_{q,p}}{\Sigma_q^2}\right] \tag{21}$$

where $\gamma_{q,p}$ is given by $\sqrt{\mu_{q,p}^2(c) + \mu_{q,p}^2(s)}$ and Σ_q^2 is given by (20). From Theorem 1, the overall pdf (or histogram) of the envelope derived from the $4NQ$ samples of $\tilde{s}(t)$ is given by

$$f_{|\tilde{s}|}(\alpha) = \frac{1}{4Q} \sum_{q=1}^{Q} \sum_{p=1}^{4} f_{q,p}(\alpha). \tag{22}$$

To derive the peak envelope according to the probabilistic definition in (1), we consider

$$\begin{aligned} P_c &= \Pr[|\tilde{s}| > \alpha_0] \\ &= 1 - \int_0^{\alpha_0} f_{|\tilde{s}_q|}(\alpha)\, d\alpha \\ &= \frac{1}{4Q} \sum_{q=1}^{Q} \sum_{p=1}^{4} \left\{\mathcal{M}_1\left[\frac{\gamma_{q,p}}{\Sigma_q}, \frac{\alpha_0}{\Sigma_q}\right]\right\} \end{aligned} \tag{23}$$

where $\mathcal{M}_1(a, b)$ is the Marcum's function given by

$$\mathcal{M}_1(a, b) = e^{-(a^2+b^2/2)} \sum_{k=0}^{\infty} \frac{a^k}{b} I_k(ab). \tag{24}$$

Note that, since $\tilde{x}_i(t)$ is a low-pass random process, the combined signal power Σ^2 is given by

$$\begin{aligned}\Sigma^2 &\stackrel{\text{def}}{=} \frac{1}{N} \sum_{n=1}^{N} |\tilde{s}[n]|^2 \\ &= \frac{1}{4Q} \sum_{q=1}^{Q} \sum_{p=1}^{4} [\mu_{q,p}^2(c) + \mu_{q,p}^2(s) + 2\Sigma_q^2] \\ &= 4N_c\psi_0^2 + 2N_c\sigma_0^2 \\ &= 4N_c \sum_{m=0}^{N_u-1} \psi_m^2. \end{aligned} \tag{25}$$

Therefore, the PAR of the multicarrier signal is given by

$$\text{PAR}(P_c) = 20 \log_{10}\left\{\frac{\alpha_0}{\Sigma}\right\} (\text{dB}). \tag{26}$$

To verify the closeness of the analytical results, we considered combining three[6] DS-CDMA baseband signals, each modulated by $\omega_1, \omega_2, \omega_3$, respectively. The histograms obtained from simulations and (26) are compared as shown in Fig. 5. It is shown that the calculated pdf matches that obtained from simulations closely for different combining phases except at very low probability where the number of samples in the simulation is not sufficient to accurately estimate the pdf at these probability values (10^{-5}). In Fig. 6, the simulated and calculated PAR's of CDMA2000 3-carriers signal varied with respect to the combining phases ($\Delta\theta$) and traffic data correlation, ρ, is plotted with different values of pilot transmit gain. A large pilot transmit gain is used to exaggerate the variations in the PARs and to test the analytical results under extreme conditions. As shown in the Fig. 7, individual carriers are essentially uncorrelated at small pilot power where the combined signal, $\tilde{s}(t)$, becomes stationary and the envelope-pdf becomes Rayleigh distributed and hence independent of the combining phases. It can be seen that the simulated PARs fall within 0.05 dB of the calculated PARs for most of pilot transmit gain and $\delta\theta$. Furthermore, the difference in PARs between using the best walsh codes and the worst walsh codes vanished in the multi-carrier situation. This could be explained by the fact that without loss of generality, the combined 3-carriers baseband signal, $\tilde{s}(t)$, is given by (27) when the middle carrier frequency is factorized out.

$$\tilde{s}(t) = \tilde{x}_1(t)e^{-j(2\pi\Delta ft+\theta_1)} + \tilde{x}_2(t) + \tilde{x}_3(t)e^{j(2\pi\Delta ft+\theta_3)}. \tag{27}$$

Since Δf is the carrier spacing which is approximately equal to the chip frequency, any peak variations due to the effect of walsh code combinations (as described in Section III) would be smoothed out by the term $e^{\pm j(2\pi\Delta ft+\theta)}$. A peak will show up only when the sub-chip interval (corresponding to the peak) aligns with the time when $e^{\pm j(2\pi\Delta ft+\theta)} = 1$ which is quite unlikely in probability. Therefore, the walsh code dependency of PAR vanished in multicarrier systems.

Moreover, it is important to distinguish the effect of sharing a common pilot between different carriers and the effect of *traffic data* correlations on the PAR. For the case without traffic data correlations between different carriers ($\rho = 0$), we observe from Fig. 6 that the multi-carrier combined PAR is actually lower than the PAR before combining. This could be explained by the last paragraph that the sinusoidal term actually smooth out the peaks of the baseband signals and $\Sigma_q = \Sigma \; \forall \; q$. In the extreme case, when we have a very high power pilot, the combined signal is very close to a sinusoid and the PAR for a sinusoid is well known to be much lower than the PAR of a Gaussian-like process [10], [11]. This explains the lower PAR after multi-carrier combining. On the other hand, when there is traffic data correlations ($\rho \neq 0$), the combined PAR is higher than the PAR

[6]To better illustrate the results, 3-carrier is chosen. This is because 3-carrier is a common setting in CDMA2000 with 5-MHz bandwidth.

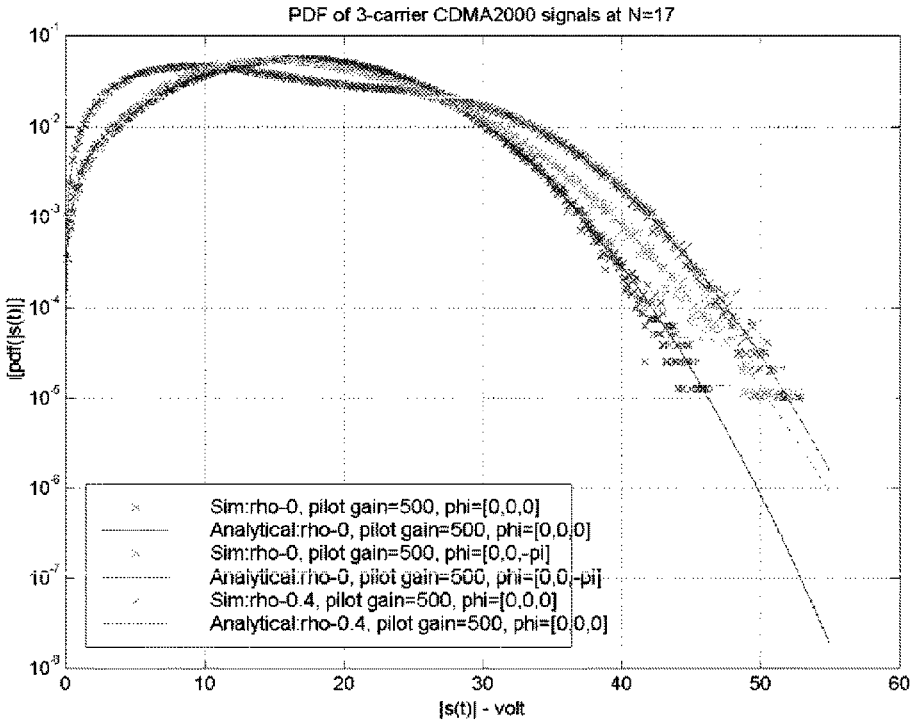

Fig. 5. Histograms of CDMA2000 three-carriers DS-CDMA signal envelope simulations and analytical results in log-scale. "x" denotes simulation results while the line represents analytical results.

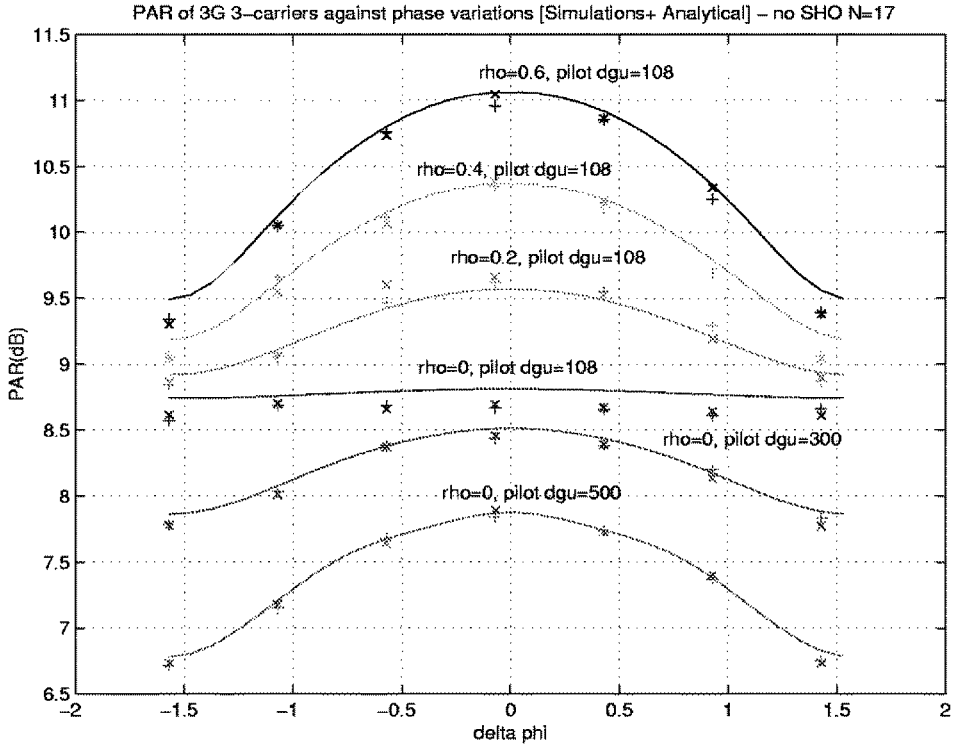

Fig. 6. Comparison of calculated PAR's and simulated PAR's for a CDMA2000 3-carriers DS-CDMA signal using pilot dgu = [108, 300, 500], paging dgu = 64, sync dgu = 34, nominal dgu = 73.4 and rho = [0, 0.6] with 17 users. "+" and "x" corresponds to the simulated PARs for $W_{\min}$ and $W_{\max}$ walsh sets respectively. "dgu" is the unit corresponding to the amplifier gain applied. $P_c = 0.99$.

before multicarrier combining. This is because the total signal power, Σ^2, is unchanged from (24) but there exist some $\Sigma_q > \Sigma$ which causes a rise in the tail part of the combined Rician distribution, creating a higher PAR. For example, at $\rho = 0.2$, the

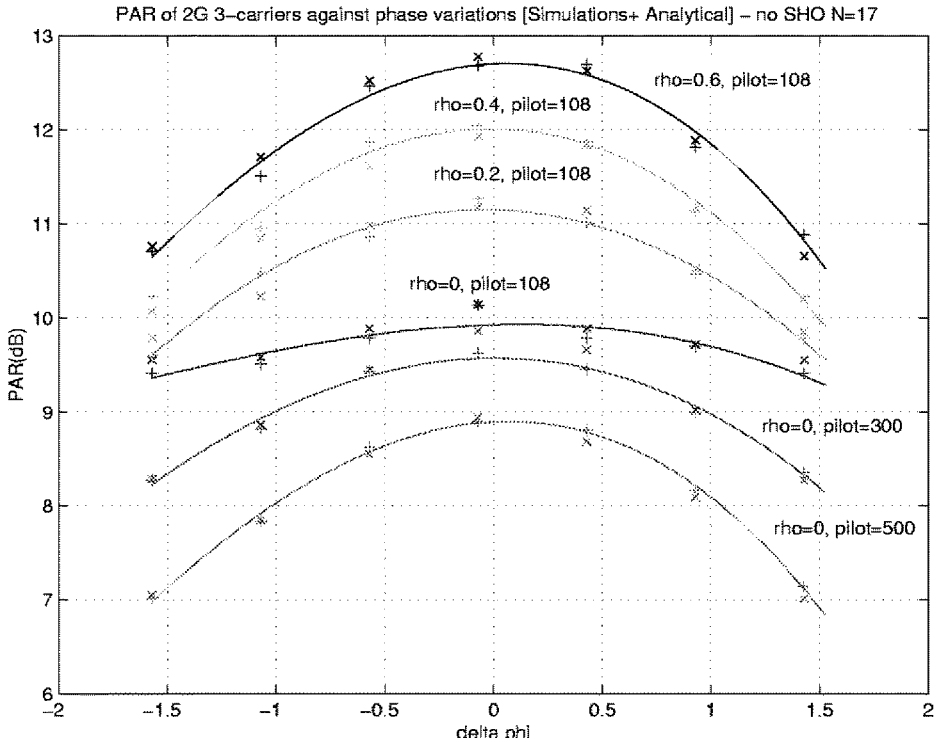

Fig. 7. Comparison of calculated PARs and simulated PARs for a IS95 3-carriers DS-CDMA signal using pilot dgu = [108, 300, 500], paging dgu = 64, sync dgu = 34, nom dgu = 73.4, rho = [0, 0.6] with 17 users. "+" and "x" correspond to simulated PARs using $W_{\max}$ and $W_{\min}$ respectively. "dgu" refers to the transmitter gain applied to the channels. $P_c = 0.99$.

rise in PAR after multicarrier combining reaches 1 dB. This suggested the reasons why an increase in PAR of multicarrier CDMA systems has been reported in field test. In [7], it was found out that the traffic data bits used to measure the PAR is actually highly correlated and the long code mask for each traffic channel is turned off, causing a high traffic data correlations between carriers.

Finally, because of the close match between the analytical and the simulation results, (26) could be used to optimize the PAR without doing costly simulations. This is elaborated more on Section V.

B. Application to IS95 DS-CDMA

Following similar technique as in Section IV-A, the common pilot signal is taken out of each baseband signal. The real and imaginary parts of the N samples in subset-(q, p) are given by

$$\begin{aligned}\Re[\tilde{s}_{q,p}(n)] &= \psi_0 \sum_{i=1}^{N_c} \left[PN_I(t_{q,p,n}) \cos\left(\frac{2\pi P_i q}{Q_i} + \theta_i\right) \right. \\ &\qquad \left. - PN_Q(t_{q,p,n}) \sin\left(\frac{2\pi P_i q}{Q_i} + \theta_i\right) \right] \\ &\quad + \sum_{i=1}^{N_c} \left[\tilde{x}'_{i,c}(t_{q,p,n}) \cos\left(\frac{2\pi P_i q}{Q_i} + \theta_i\right) \right. \\ &\qquad \left. - \tilde{x}'_{i,s}(t_{q,p,n}) \sin\left(\frac{2\pi P_i q}{Q_i} + \theta_i\right) \right] \\ &= \mu_{q,p}(c) + \Re[\tilde{s}'_{q,p}(t_{q,p,n})] \end{aligned} \tag{28}$$

$$\begin{aligned}\Im[\tilde{s}_{q,p}(n)] &= \psi_0 \sum_{i=1}^{N_c} \left[PN_Q(t_{q,p,n}) \cos\left(\frac{2\pi P_i q}{Q_i} + \theta_i\right) \right. \\ &\qquad \left. + PN_I(t_{q,p,n}) \sin\left(\frac{2\pi P_i q}{Q_i} + \theta_i\right) \right] \\ &\quad + \sum_{i=1}^{N_c} \left[\tilde{x}'_{i,s}(t_{q,p,n}) \cos\left(\frac{2\pi P_i q}{Q_i} + \theta_i\right) \right. \\ &\qquad \left. + \tilde{x}'_{i,c}(t_{q,p,n}) \sin\left(\frac{2\pi P_i q}{Q_i} + \theta_i\right) \right] \\ &= \mu_{q,p}(s) + \Im[\tilde{s}'_{q,p}(t_{q,p,n})]. \end{aligned} \tag{29}$$

Because of BPSK, the I and Q channel shares the same data bits for each carrier and hence $\Re[\tilde{x}'_{i,c}]$ and $\Im[\tilde{x}'_{i,s}]$ are heavily correlated. Furthermore, to illustrate the effect of traffic channel bits correlation on PAR, we assume $\Re[\tilde{x}'_{i,c}]$ and $\Im[\tilde{x}'_{j,s}]$ are correlated as well. Define σ_0^2 and ρ as

$$\sigma_0^2 \stackrel{\text{def}}{=} \mathcal{E}[(\Re(\tilde{x}'_i))^2] = \mathcal{E}[(\Im(\tilde{x}'_i))^2] = \sum_{m=1}^{N_u-1} \psi_m^2 \tag{30}$$

$$\begin{aligned}\rho &\stackrel{\text{def}}{=} \frac{1}{\sigma_0^2} \mathcal{E}[(\Re(\tilde{x}'_i))(\Re(\tilde{x}'_j))] = \mathcal{E}[(\Im(\tilde{x}'_i))(\Im(\tilde{x}'_j))] \\ &= \sum_{m=1}^{N_u-1} \psi_m^2 \langle w_m^{(i)} w_m^{(j)} \rangle \langle d_m^{(i)} d_m^{(j)} \rangle. \end{aligned} \tag{31}$$

The 2nd order statistics of $\tilde{x}'_i$ are given by

$$\mathcal{E}[(\Re(\tilde{x}'_i))^2] = \mathcal{E}[(\Im(\tilde{x}'_i))^2] = \sigma_0^2 \tag{32}$$

$$\mathcal{E}[(\Re(\tilde{x}'_i))(\Im(\tilde{x}'_i))] = \sigma_0^2 PN_I PN_Q \tag{33}$$

$$\mathcal{E}[(\Re(\tilde{x}'_i))(\Re(\tilde{x}'_j))] = \mathcal{E}[(\Im(\tilde{x}'_i))(\Im(\tilde{x}'_j))] = \sigma_0^2 \rho \tag{34}$$

$$\mathcal{E}[(\Re(\tilde{x}'_i))(\Im(\tilde{x}'_j))] = \mathcal{E}[(\Im(\tilde{x}'_i))(\Re(\tilde{x}'_j))] = \sigma_0^2 \rho PN_I PN_Q. \tag{35}$$

$\Re[\tilde{s}_{q,p}(n)]$ and $\Im[\tilde{s}_{q,p}(n)]$ are modeled by zero-mean Gaussian processes and their 2nd order statistics are given by

$$\begin{aligned}\Sigma_{q,p}^2(c) &\stackrel{\text{def}}{=} \mathcal{E}[\Re(\tilde{s}'_{q,p})^2] \\ &= \sigma_0^2 \sum_{i=1}^{N_c} \left(1 - PN_I PN_Q \sin\left(4\pi q \frac{P_i}{Q_i} + 2\theta_i\right)\right) \\ &\quad + \sigma_0^2 \rho \sum_{i=1}^{N_c} \sum_{\substack{j=1 \\ i \neq j}}^{N_c} \\ &\quad \cdot \left[\cos\left(2\pi q\left(\frac{P_i}{Q_i} - \frac{P_j}{Q_j}\right) + (\theta_i - \theta_j)\right) - PN_I \right. \\ &\quad \left. \cdot PN_Q \sin\left(2\pi q\left(\frac{P_i}{Q_i} + \frac{P_j}{Q_j}\right) + (\theta_i + \theta_j)\right)\right]\end{aligned} \tag{36}$$

$$\begin{aligned}\Sigma_{q,p}^2(s) &\stackrel{\text{def}}{=} \mathcal{E}[\Im(\tilde{s}'_{q,p})^2] \\ &= \sigma_0^2 \sum_{i=1}^{N_c} \left(1 + PN_I PN_Q \sin\left(4\pi q \frac{P_i}{Q_i} + 2\theta_i\right)\right) \\ &\quad + \sigma_0^2 \rho \sum_{i=1}^{N_c} \sum_{\substack{j=1 \\ i \neq j}}^{N_c} \\ &\quad \cdot \left[\cos\left(2\pi q\left(\frac{P_i}{Q_i} - \frac{P_j}{Q_j}\right) + (\theta_i - \theta_j)\right) + PN_I \right. \\ &\quad \left. \cdot PN_Q \sin\left(2\pi q\left(\frac{P_i}{Q_i} + \frac{P_j}{Q_j}\right) + (\theta_i + \theta_j)\right)\right]\end{aligned} \tag{37}$$

$$\begin{aligned}\Gamma_{q,p}^2 &\stackrel{\text{def}}{=} \mathcal{E}[\Re(\tilde{s}'_{q,p})\Im(\tilde{s}'_{q,p})] \\ &= \sigma_0^2 PN_I PN_Q \sum_{i=1}^{N_c} \cos\left(4\pi q \frac{P_i}{Q_i} + 2\theta_i\right) \\ &\quad + \sigma_0^2 \rho \sum_{i=1}^{N_c} \sum_{\substack{j=1 \\ i \neq j}}^{N_c} \\ &\quad \cdot \left[PN_I PN_Q \cos\left(2\pi q\left(\frac{P_i}{Q_i} + \frac{P_j}{Q_j}\right) + (\theta_i + \theta_j)\right) \right. \\ &\quad \left. + \sin\left(2\pi q\left(\frac{P_j}{Q_j} - \frac{P_i}{Q_i}\right) + (\theta_j - \theta_i)\right)\right].\end{aligned} \tag{38}$$

Since the envelope square is given by

$$|\tilde{s}_{q,p}|^2 = [\mu_{q,p}(c)^2 + \Re(\tilde{s}'_{q,p})]^2 + [\mu_{q,p}(s)^2 + \Im(\tilde{s}'_{q,p})]^2$$

and $\Re(\tilde{s}'_{q,p})$ and $\Im(\tilde{s}'_{q,p})$ are correlated, the pdf of $|\tilde{s}_{q,p}|^2$ is no longer a chi square. It is shown that the pdf is given by [12]

$$f_{q,p}(\beta) = \frac{1}{2\pi} \int_{-\infty}^{\infty} \Phi_{q,p}(jv) e^{-jv\beta}\, dv \tag{39}$$

where $\Phi_{q,p}(\beta)$ is the characteristic function of the pdf. From Theorem 1 again, the peak-square envelope, $\beta_0 = \alpha_0^2$ at probability P_c is given by the solution to

$$P_c = 1 - \frac{1}{8\pi Q} \sum_{q=1}^{Q} \sum_{p=1}^{4} \int_{-\infty+j\epsilon}^{\infty+j\epsilon} \frac{\Phi_{q,p}(jv)[1 - e^{-jv\beta_0}]}{jv}\, dv. \tag{40}$$

Similar to (25), the total signal power of $\tilde{s}(t)$ is given by

$$\begin{aligned}\Sigma^2 &= \frac{1}{4Q} \sum_{q=1}^{Q} \sum_{p=1}^{4} (\mu_{q,p}^2(c) + \mu_{q,p}^2(s) + \Sigma_q^2(c) + \Sigma_q^2(s)) \\ &= 2N_c \sum_{m=0}^{N_u - 1} \psi_m^2.\end{aligned} \tag{41}$$

A comparison of simulated and calculated PARs for IS95 3-carriers system at various ρ and pilot transmit gain is shown in Fig. 7. Similar observations are found with respect to the behavior of PAR.

C. Comparison Between IS95 and CDMA2000 Multicarrier Systems

As a conclusion to this section, the change of PAR in multicarrier systems is due to the loss of ergodicity in the combined signal. For a CDMA2000 multicarrier system, the loss of ergodicity is due to the common pilot and traffic data correlation in each carrier. For a IS95 multicarrier system, the loss of ergodicity is due to the common pilot, traffic data correlation and the high correlation (in magnitude) between the I and Q components.[7] For this reason, PAR of IS95 systems is higher than the CDMA2000 systems at the same condition in multicarrier environment.

Another important observation is that multicarrier PAR does not depend on walsh code combinations of individual carrier anymore in both the IS95 and CDMA2000 systems (compared to the single carrier situation in Section III). When traffic data symbols are uncorrelated, the combined PAR is actually lower than the PAR of the baseband signal.

V. PAR Control Methods

As mentioned in Section I, a large backoff factor is needed to accommodate the forward link CDMA signal with a large PAR. This effectively reduces the allowable average transmit

[7]The correlation between I and Q signal for a IS95 system is due to BPSK modulation.

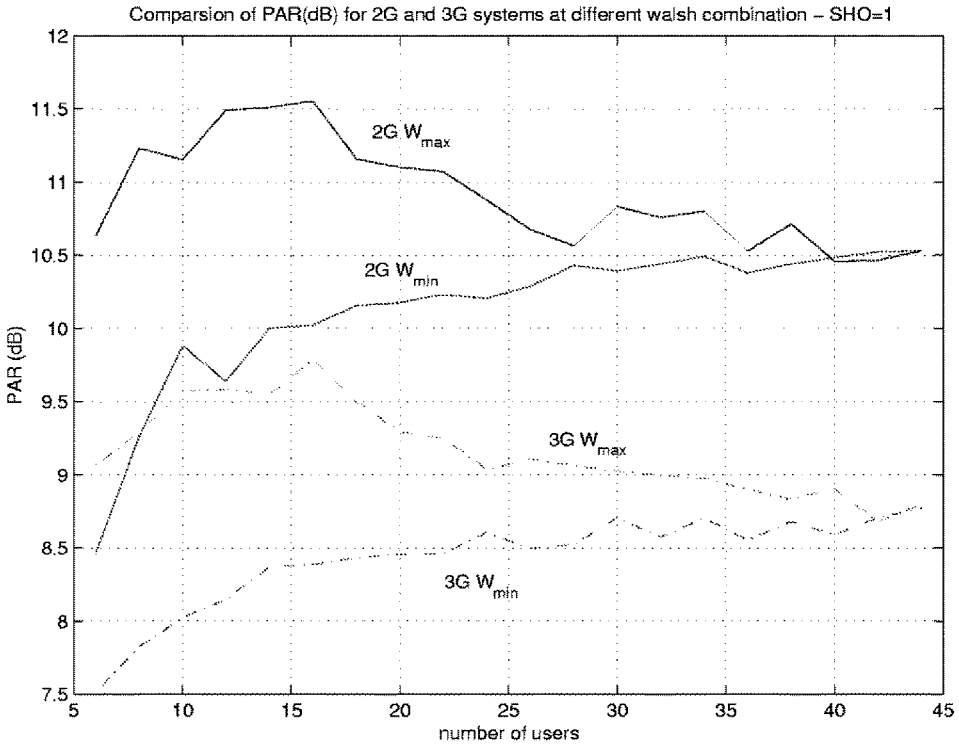

(a)

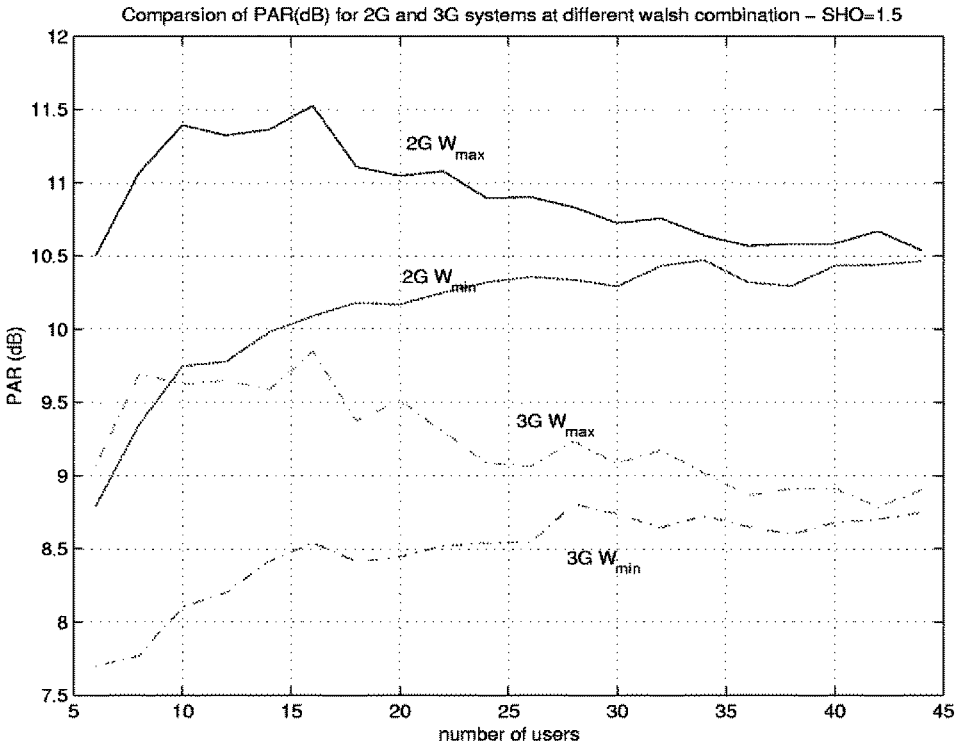

(b)

Fig. 8. Static comparison of PAR for IS95 and CDMA2000 systems with $\mathcal{W}_{\max}$, $\mathcal{W}_{\min}$ and N_u as variables. 2G represents the IS95 2nd generation systems and 3G represents the CDMA2000 3rd generation systems.

power for a given linear power amplifier. Therefore, it would be desirable to reduce the PAR of the CDMA forward link signal.

In general, PAR control schemes could be classified as

1) synthesis technique;
2) predistortion technique.

The *synthesis techniques* will be described in details in this section. The *predistortion technique* is currently under investigation.

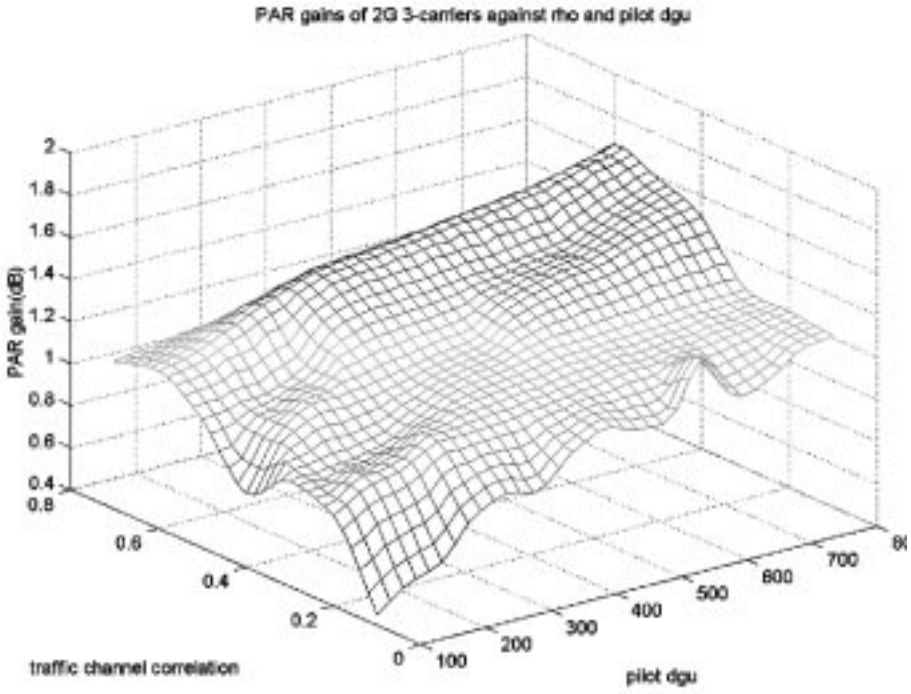

(a)

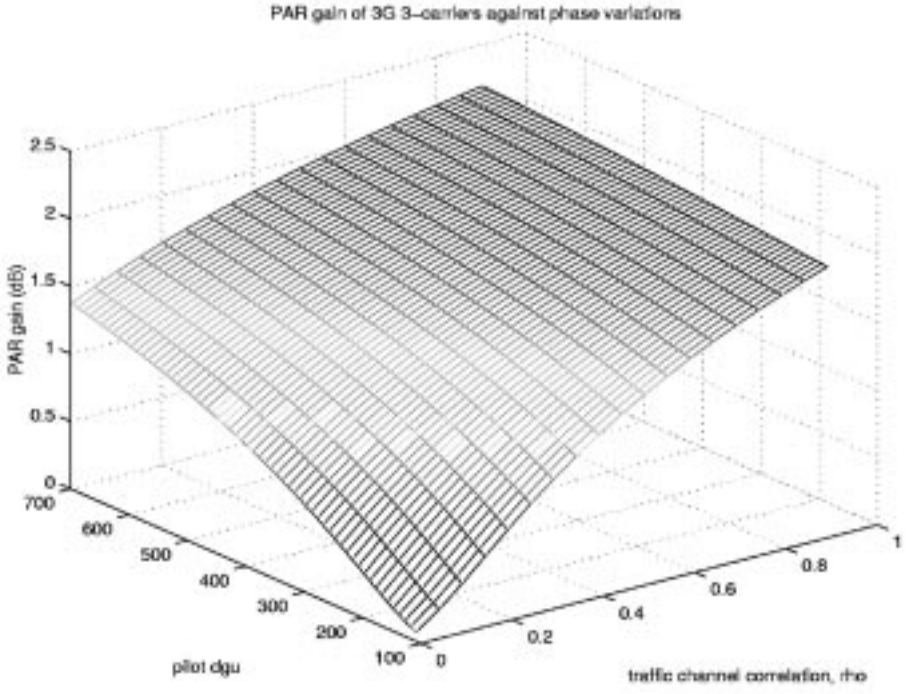

(b)

Fig. 9. PAR gain for CDMA2000 and IS95 3-carriers systems with respect to pilot dgu (ψ_0) and traffic channel correlation (ρ). DGU represents the transmit gains applied to the channels at the base-station.

A. Synthesis PAR Reduction Technique for Single Carrier

As its name implies, the synthesis PAR reduction schemes try to manipulate on the *source data* or parameters in the synthesis of the transmit signal so as to reduce the inherit PAR. Several schemes have been proposed in [13], [3], and [14] to deal with the PAR of OFDM signal by selective mapping or redundancy coding. For single carrier DS-CDMA signal, the PAR is determined by the *transmit digital sequence*, $\lambda_i^{(I)}$

and $\lambda_l^{(Q)}$. From (3)

$$\lambda_l^{(I)} = \sum_{n=0}^{N_u-1} d_n^{(I)} w_n(l), \quad \lambda_l^{(Q)} = \sum_{n=0}^{N_u-1} d_n^{(Q)} w_n(l). \quad (42)$$

As shown in (42), we could either manipulate the data bits $\{d_n^{(I)}, d_n^{(Q)}\}$ or the walsh codes $\{w_n(l)\}$ to control $\lambda_l^{(I)}$ and $\lambda_l^{(Q)}$. The simplest way is to selectively assign walsh codes to each user so as to minimize the PAR because it does not require changes in the mobile station (MS) receiver. This is band limited in the next subsection.

1) Selective Walsh Code Assignment: Due to the limited transmitted bandwidth, there will be *inter-chip interference* due to the transmit pulse width spanning more than one chip interval. Assume that the transmit pulse, $p(t)$, spans $2L + 1$ chip-intervals. On each chip-interval, we over-sample the pulse by K times. (i.e., there are K samples (subchips) of transmit pulse, $p(t)$, on each chip). Without loss of generality, we consider the peak of either the I-signal or the Q-signal. Let $S_{N_u}(k, l)$ be the magnitude of the envelope of the I or Q signal at the kth *subchip* between $t = lT_c$ and $t = (l + 1)T_c$. It is given by

$$\begin{aligned} S_{N_u}(k, l) &= \sum_{l'=-L}^{L} \lambda_{l+l'} PN_{l+l'} p\left[\frac{(l - l'K)T_c}{K}\right] \\ &= \sum_{l'=-L}^{L} \lambda_{l+l'} PN_{l+l'} p_{k-l'K}. \end{aligned} \quad (43)$$

For any given set of walsh codes, $\mathcal{W}_{N_u} = \{w_{n_1}, w_{n_2}, \ldots, w_{n_{N_u}}\}$, there exist a unique set of data bits $\mathcal{D}_{N_u} = \{d_1^*, d_2^*, \ldots, d_n^*\}$ such that $\lambda_l = N_u$. Since $PN_l \in [1, -1]$, the *worst-case peak* of the envelope (43) between $t = lT_c$ and $t = (l + 1)T_c$ is given by

$$S_{N_u}^*(l) = \max_{k \in [0, K-1]} \left[\sum_{l'=-L}^{L} |\lambda_{l+l'} p_{k-l'K}|\right] \quad (44)$$

The problem is formulated as follows.

To minimize the worst case peak $S_{N_u}^* = \max_{l \in [0, M-1]}[S_{N_u}^*(l)]$ over the set of walsh codes, $\mathcal{W}_{N_u}$, for N_u users with the constraint

$$\mathcal{W}_{N'} \subset \mathcal{W}_{N'+1}, \qquad N' \in [1, 2, \cdots, N_u - 1] \quad (45)$$

where M is the number of chips per coded bit (i.e., $M = T_b/T_c$). The constraint is needed because we want to keep the peak to be minimal for all N as new users are added into the system.

This optimization problem is solved sequentially and the following is the result of computer search.

The set of walsh codes that gives a minimal worse case peak, $S_{N_u}^*$, for $N_u = 1 - 17$ is sorted as $\mathcal{W}_{\min} = \{w_0, w_{32}, w_1, w_{27}, w_{25}, w_{13}, w_{26}, w_{20}, w_{14}, w_{15}, \ldots\}$. For the sake of comparison, the set of walsh codes that gives a maximal worst-case peak is given by $\mathcal{W}_{\max} = \{w_0, w_{32}, w_4, w_{24}, w_{40}, w_{48}, w_8, w_{16}, w_{56}, w_{13}, \cdots\}$. Fig. 8 shows the difference in PAR(dB) of the IS95 and CDMA2000 signals resulting from $\mathcal{W}_{\min}$ and $\mathcal{W}_{\max}$ respectively.

As shown in the Fig. 8(a), there is 1.5–2 dB PAR difference between the system using $\mathcal{W}_{\min}$ and $\mathcal{W}_{\max}$ walsh code for the IS95 and CDMA2000 systems. Furthermore, given the same walsh code, there is a 1.5–2.5 dB reduction of PAR for CDMA2000 system when N is around 16. As the number of users per sector increases, the difference between the PARs of the $\mathcal{W}_{\max}$ and $\mathcal{W}_{\min}$ decreased. This is because the transmit signal approaches a Gaussian distribution as N_u increases. Since the pdf (histogram) of a Gaussian signal is fixed, the PAR difference tends to vanish.

When an MS is in soft handoff, the transmit power of the forward-link power control bits is increased by a certain factor (SHO factor) to compensate for the drop in transmit power of the traffic channel.[8] Fig. 8(b) shows the difference in PAR when SHO factor $= 1.5$ is included. Similar PAR differences are observed.

In current IS95 systems, the normal loading of a sector is about 14 users.[9] Therefore, the selective walsh code mapping method could contribute to 1–2 dB reduction in PAR.

B. Synthesis PAR Reduction Technique for Multi-Carrier System

As shown in Fig. 6, the PAR of 3-carrier system is not affected by the selection of walsh codes. For example, at $\delta\theta = 0$, the PAR difference between the best walsh code and the worst walsh codes (in single carrier sense) is less than 0.05 dB. As discussed in Section IV, the control parameters for the PAR in multi-carrier system are the combining phases, $[\theta_1, \theta_2, \theta_3]$. In this section, we study the effectiveness of reducing the PAR by adjusting the combining phases.

For a CDMA2000 multi-carrier system, PAR is determined (26). Therefore, the best case and the worst case combining phases are found by optimizing (26) with respect to the combining phases. Similarly optimization is performed on (40) for IS95 systems.

Fig. 9 shows the PAR gain[10] of IS95 and CDMA2000 3-carrier systems with respect to the pilot dgu, ψ_0. As shown in Fig. 9, there is essentially little PAR gain at low ψ_0. As shown in Fig. 9, the PAR gains are negligible at low pilot transmit gain and low traffic channel correlation (ρ).

VI. Conclusion

In this paper, we have discussed the PAR for the single carrier and multi-carrier IS95 and CDMA2000 systems. Analytical expressions are formulated to approximate the histogram and PAR

[8]Power control bits are not combined between Soft handoff legs and hence they need to be transmitted at a higher power to compensate for the reduction in the forward link transmitted power due to power control.

[9]Although we have 64 walsh channels in the forward link, the maximum number of supported users is much less than 64. This is because the number of users is constrained by the reverse link capacity as well as the base station transmit power.

[10]PAR gain refers to the difference between the best phases and the worst phases.

of the multi-carrier cases for both IS95 and CDMA2000 systems. Analytical results closely matched the simulation results. In the process of deriving the expressions, a better insight on the reasons of PAR variations could be obtained. Finally, an algorithm to optimally select walsh codes (in PAR sense) have been proposed and its impact on PAR is discussed. The following are the main conclusions found.

1) PARs of CDMA2000 system are smaller than IS95 system both in the single carrier and multi-carrier situations due to QPSK modulation and complex spreading.
2) PAR dependency of walsh code for single carrier systems is due to the fact that transmit pulse spans over more than one chip interval.
3) PAR reduction between the best and the worst walsh code sets reaches 1.5–2 dB at 14 users in *static* analysis. PAR variations with respect to walsh code sets vanished in multi-carrier systems both for IS95 and CDMA2000 systems.
4) At low pilot transmit gain and traffic channel correlation, the PAR gain of combining phases adjustment is less than 0.3 dB for IS95 and CDMA2000 multi-carrier systems.
5) When traffic data bits (or assigned walsh codes) are uncorrelated between different carriers, the PAR of the multicarrier combined signal is lowered than the baseband PAR. On the other hand, when data bits are correlated, combined PAR raised.

In fact, a potential problem for the third generation systems is the problems of PAR when very high data rates with a small number of users, low processing gain, low statistical multiplexing and short spreading codes are employed. The analytical model in this paper could be applied to analyze such scenario. However, the challenge lies in finding an analytical model for the pdf of SC CDMA2000 signals when the number of users is small, and this is under further investigation.

ACKNOWLEDGMENT

The author would like to thank M. Meyers and the CDMA2000 performance analysis group at Lucent Technologies for the motivation behind this work.

REFERENCES

[1] M. Pauli and H. Kuchenbecker, "On the reduction of the out-of-band radiation of OFDM signals," in *Proc. ICC'98*, Alanta, GA, USA, June.
[2] M. Friese, "Multitone signals with low crest factor," *IEEE Trans. Commun.*, vol. 45, pp. 1338–1344, Oct. 1997.
[3] S. Shepherd, J. Orriss, and S. Barton, "Asymptotic limits in peak envelope power reduction by redundant coding in orthogonal frequency-division multiplex modulation," *IEEE Trans. Commun.*, vol. 46, pp. 5–10, Jan. 1998.
[4] J. A. Davis and J. Jedwab, "Peak-to-mean power control and error correction for OFDM transmission using Golay sequences and Reed–Muller codes," *Elect. Lett.*, vol. 33, pp. 267–268, Feb. 1997.
[5] M. Friese, "OFDM signals with low crest-factor," in *Proc. Globecom97*, pp. 290–294.
[6] S. H. Muller and J. B. Huber, "A novel peak-power reduction scheme for OFDM," in *Proc. PIMRC 97*, pp. 1090–1094.
[7] Z. Ma, H. Wu, and P. Polakos, "On the peak-to-average ratio (PAR) of CDMA signals,", Holmdel, NJ, Internal Technical Memo of Lucent Technologies, June 1998.
[8] S. Dennett, "The CDMA2000 ITU-R RTT candidate submission,", TR45.5, 1998.
[9] Z. Ma, H. Wu, and P. Polakos, "On clipping of CDMA Signals,", Holmdel, NJ, Internal Technical Memo of Lucent Technologies, June 1998.
[10] K. Fazel and S. Kaiser, "Analysis of nonlinear distortions on MC-CDMA," in *Proc. ICC'98*, Atlanta, GA, USA, June.
[11] R. Dinis and A. Gusmao, "Performance evaluation of a multicarrier modulation technique allowing strongly nonlinear amplification," in *Proc. ICC'98*, Atlanta, GA, USA, June.
[12] N. L. Johnson, *Continuous Univariate Distributions*, Second ed. New York: Wiley, 1994.
[13] A. C. Caswell, "Multicarrier transmission in a mobile radio channel," *Elect. Lett.*, vol. 32, pp. 1962–1964, Oct. 1996.
[14] S. Shepherd, J. Orriss, and S. Barton, "Simple coding scheme to reduce peak factor in QPSK multicarrier modulation," *Elect. Lett.*, vol. 31, pp. 1131–1132, July 1995.

Vincent K. N. Lau received the B. Eng. (Hons.) from the University of Hong Kong in 1992 and the Ph.D. degree from the University of Cambridge, Cambridge, U.K. in 1997.

From 1992 to 1995, he was with Hong Kong Telecom as Project Engineer and, later, System Engineer, responsible for transmissions equipment. From 1997 to 1999, he was with Lucent Technologies, Bell Labs, Holmdel, NJ as member of technical staff. He was engaged in the design and development of 3rd generation wideband CDMA (cdma2000). In 1999, he joined the Department of EEE at the University of Hong Kong, where he is currently the co-director of the 3G Technology Center and the Information Engineering Programme. His research interests include information theory, adaptive channel coding and modulation, power control and CREST factor control algorithms, and multiple access protocols wireless systems.

Dr. Lau received the Sir Edward Youde Memorial Fellowship and the Croucher Foundation Award in 1995.